Brain (2002), **125,** 2257–2271

Abnormalities of grey and white matter [^{11}C]flumazenil binding in temporal lobe epilepsy with normal MRI

A. Hammers,[1,2,3] M. J. Koepp,[1,2,3] R. Hurlemann,[2] M. Thom,[2] M. P. Richardson,[1,2,3] D. J. Brooks[1] and J. S. Duncan[1,2,3]

[1]*MRC Clinical Sciences Centre and Division of Neuroscience, Faculty of Medicine, Imperial College,* [2]*Department of Clinical and Experimental Epilepsy, Institute of Neurology, University College London, London and* [3]*National Society for Epilepsy MRI Unit, Chalfont St Peter, UK*

Correspondence to: Professor John S. Duncan, MA, DM, FRCP, National Society for Epilepsy and Institute of Neurology, 33 Queen Square, London WC1N 3BG, UK
E-mail: j.duncan@ion.ucl.ac.uk

Summary

In 20% of potential surgical candidates with refractory epilepsy, current optimal MRI does not identify the cause. GABA is the principal inhibitory neurotransmitter in the brain, and $GABA_A$ receptors are expressed by most neurones. [^{11}C]Flumazenil (FMZ) PET images the majority of $GABA_A$ receptor subtypes. We investigated abnormalities of FMZ binding in grey and white matter in 18 patients with refractory temporal lobe epilepsy (TLE) and normal quantitative MRI. Parametric images of FMZ volume of distribution (FMZ-V_d) were calculated. Twenty-one healthy controls were scanned for comparison. Statistical parametric mapping (SPM99) was used to localize significant changes in FMZ-V_d in individual patients and between groups, specifically including the entire white matter in all subjects through explicit masking. Sixteen of 18 patients showed single or multiple abnormalities of FMZ-V_d. Six had hippocampal decreases of FMZ-V_d. Eleven patients showed increased FMZ-V_d in the temporal lobe white matter (TLWM). Outside the mesial temporal structures, seven showed multiple areas of increase or decrease and only one a single area of decrease. In seven of the 16 patients with abnormalities, findings were concordant with EEG and clinical data, enabling further presurgical evaluation. Group findings were: (i) decreased FMZ-V_d in the ipsilateral (Z = 3.01) and contralateral (Z = 2.56) hippocampus; (ii) increased FMZ-V_d in the ipsilateral (Z = 3.71) and contralateral TLWM (two clusters, Z = 3.11 and 2.79); and (iii) increased FMZ-V_d in the ipsilateral frontal lobe white matter between the superior and medial frontal gyrus (Z = 3.80) with similar changes contralaterally (Z = 4.87). No changes were found in the thalamus and basal ganglia. Region-of-interest analyses indicated an average increase in FMZ binding of 16% in the TLWM ipsilateral to the epileptic focus. PET findings were corroborated by invasive EEG or pathology in five cases. FMZ–PET, analysed by SPM with explicit masking, was sensitive in patients with normal MRI, and hippocampal abnormalities were detected in a third of these patients. Furthermore, increases in FMZ binding in TLWM, indicating microdysgenesis, were detected in the majority of these patients and may represent the structural basis of their epilepsy.

Keywords: PET; SPM99; temporal lobe epilepsy; flumazenil binding

Abbreviations: FLWM = frontal lobe white matter; FMZ = flumazenil; FMZ-V_d = flumazenil volume of distribution; FWHM = full width half maximum; SPM = statistical parametric mapping; TLE = temporal lobe epilepsy; TLWM = temporal lobe white matter

Introduction

In patients with medically refractory partial seizures, surgery offers the possibility of lasting suppression of seizures. The majority of patients referred for epilepsy surgery have temporal lobe epilepsy (TLE), and 60% of these have hippocampal sclerosis (Babb *et al*., 1984). MRI has been reported to be normal in 15–30% of

patients with TLE, even when histopathological examination of resected specimens detects hippocampal sclerosis, focal cortical dysplasia or other pathologies (Chugani *et al*., 1990; Kuzniecky *et al*., 1991; Desbiens *et al*., 1993; Van Paesschen *et al*., 1997). In the absence of identifiable pathology on imaging, surgery in TLE patients has a less favourable outcome (Berkovic *et al*., 1995). Thus, while patients with TLE and normal MRI represent a relatively large and important group in epilepsy centres, they are less likely to undergo surgery.

γ-Aminobutyric acid (GABA) is the principal inhibitory neurotransmitter in the brain, acting at the $GABA_A$ receptor complex. Flumazenil (FMZ) is a specific, reversibly bound high-affinity neutral antagonist at the benzodiazepine site of the $GABA_A$ receptor (Olsen *et al*., 1990), expressed by most neurones. [^{11}C]FMZ provides a useful *in vivo* marker of $GABA_A$ receptor binding (Maziere *et al*., 1984).

In TLE, we have shown, using partial volume effect-corrected FMZ–PET, that FMZ binding is reduced over and above hippocampal volume loss in hippocampal sclerosis (Koepp *et al*., 1997*b*). Correlation analysis of autoradiography and quantitative neuropathology in resected hippocampi also revealed a greater reduction in FMZ binding than in neuronal cell density (Hand *et al*., 1997) and good correlation between *in vivo* [^{11}C]FMZ–PET and [^{3}H]FMZ autoradiography (Koepp *et al*., 1998). These results suggest that [^{11}C]FMZ–PET may be more sensitive than MRI in the identification of subtle hippocampal abnormalities, and therefore clinically useful when MRI is unremarkable.

Malformations of cortical development are increasingly recognized as underlying medically intractable epilepsy (Kuzniecky and Jackson, 1998). Microdysgenesis, a minimal form of malformation of cortical development, is not detectable on conventional MRI and a common form is an increased density of heterotopic neurones in the white matter (Raymond *et al*., 1995). We have recently demonstrated a strong and highly significant correlation between *in vivo* temporal lobe white matter (TLWM) FMZ binding and white matter neurone number in patients with hippocampal sclerosis who underwent anterior temporal lobe resection (Hammers *et al*., 2001*a*). FMZ–PET is uniquely suited to the study of microdysgenesis in white matter due to its highly specific binding to neurones and the resulting high contrast-to-noise ratio. Previous PET studies of patients with TLE and normal MRI have not considered FMZ binding to $GABA_A$ receptors in the white matter.

The aims of the present study were to: (i) determine the ability of FMZ–PET to localize abnormalities in TLE patients with normal, high-resolution, quantitative MRI, using a more advanced version of statistical parametric mapping (SPM99) than previously (Koepp *et al*., 2000) in a different and larger series of patients; (ii) investigate with SPM99 whether TLWM FMZ binding in these patients is increased, using explicit masking; and (iii) assess common abnormalities using group comparisons.

Material and methods

Patients and controls

We studied 18 patients (11 women) with medically refractory TLE. The diagnosis and focus lateralization was based on a comprehensive assessment. This included seizure semiology obtained from eye witnesses or video recordings, interictal EEG abnormalities in all, ictal video–EEG findings in 10 patients (Table 1) and detailed neuropsychological assessment. The patients were recruited from the epilepsy clinics of the National Hospital for Neurology and Neurosurgery, Queen Square, London, UK, and the National Society for Epilepsy, Chalfont St Peter, UK. The median age at onset of habitual seizures was 19 years (range 7–54 years), the median duration of epilepsy before the PET examination was 13 years (range 1–34 years) and the median age at PET examination was 37 years (range 17–64 years). No patient had a history of prolonged febrile convulsions. Patients had a median of 62 complex partial seizures per year (range 4–1270). The antiepileptic medications were lamotrigine (11 patients), phenytoin (7), carbamazepine (5), topiramate (3), vigabatrin (2), sodium valproate (2) and gabapentin (1). Most patients received a combination of two antiepileptic drugs; one patient was not taking any medication, two were on lamotrigine monotherapy and one was on carbamazepine monotherapy. Patients who were treated with benzodiazepines or barbiturates within 2 months of the PET examination were not included in the study as these drugs could possibly interfere with [^{11}C]FMZ binding. Vigabatrin has been shown not to influence benzodiazepine binding (Verhoeff *et al*., 1999; Hammers *et al*., 2001*b*).

Twenty-one healthy volunteers (three women) were studied for comparison. The median age at examination was 31 years (range 20–71 years). They had no history of neurological or psychiatric disorder, were on no medication and had normal MRI studies.

Individuals did not consume alcohol within the 48 h preceding PET.

Written informed consent was obtained in all cases according to the Declaration of Helsinki. Approval was obtained from the Joint Ethics Committee of The Institute of Neurology and The National Hospital for Neurology and Neurosurgery, the Ethics Committee, Imperial College, Hammersmith Hospital and the UK Administration of Radiation Substances Advisory Committee (ARSAC).

Clinical data for all 18 patients are shown in Table 1. At the time of writing, four patients have undergone epilepsy surgery (Patients 8, 15, 17 and 18) and one (Patient 7) has been evaluated with depth electrodes.

PET

We used the same acquisition technique as described previously (Hammers *et al*., 2002). PET scans were performed in 3D mode with the septa retracted, using a 953B Siemens/CTI (Knoxville, TN, USA) PET camera with a

reconstructed image resolution of ~4.8 × 4.8 × 5.2 mm full width half maximum (FWHM) in air at the centre of the scanner field of view. Images were displayed as 31 transaxial planes (Bailey, 1992) with voxel sizes of 2.09 × 2.09 × 3.42 mm. Scans were acquired with transaxial planes parallel to the plane defined by the anterior and posterior commissures (AC–PC line) and coronal images orthogonal to this. A transmission scan using three rotating $^{68}Ga/^{68}Ge$-rotatory line sources was performed to enable emission scans to be corrected for attenuation. An eight-channel EEG was recorded during the PET studies to ensure that the scans were interictal. High-specific-activity [^{11}C]FMZ (370 MBq) (Maziere *et al*., 1984) was injected intravenously. Arterial blood was sampled continuously in order to determine a metabolite-corrected plasma input function (Lammertsma *et al*., 1993). A dynamic 3D series, consisting of 20 frames over 90 min, was acquired for the brain volume. A convolution subtraction scatter correction (Bailey, 1992) was used and axial scaling with the inverse of our scanner's axial profile was applied to obtain uniform efficiency throughout the field of view (Grootoonk, 1995). The 20 time frames of the dynamic image were realigned with one another by an automated least-squares technique to minimize any movement artefact during the scan (Friston *et al*., 1995*a*). Parametric images of [^{11}C]FMZ-V_d, reflecting binding to $GABA_A$ receptors at the voxel level (Koeppe *et al*., 1991), were produced from the brain uptake and plasma input functions using spectral analysis (Cunningham and Jones, 1993) with correction for blood volume.

MRI

MRIs were obtained with a 1 T scanner (Picker, Cleveland, OH, USA) using a gradient echo protocol which generated 128 contiguous 1.3 mm thick sagittal images (matrix 256 × 256 voxels, voxel size 1 × 1 × 1.3 mm, repetition time (TR) 35 ms, echo time (TE) 6 ms; flip angle 35°). These high-resolution volume-acquisition MRI scans were co-registered to the parametric images of [^{11}C]FMZ binding. In addition, all patients also had hippocampal volumetric studies with a 1.5 T GE Signa scanner (Milwaukee, WI, USA). An inversion recovery-prepared 3D spoiled gradient echo (IRP-SPGR) sequence [TR/TE/TI (inversion time)/NEX (number of excitations) 17.4/4.2/450/2, flip angle 20°, matrix size 256 × 192, field of view 24 × 18 cm] with 124 contiguous coronal slices and a slice thickness of 1.5 mm was used for volumetric studies, as described previously (Woermann *et al*., 1998). Hippocampal T_2 values were obtained as described previously (Duncan *et al*., 1996; Woermann *et al*., 1998). All MRIs were reported after the electroclinical diagnosis of TLE had been made and particular attention was paid to the temporal lobes. They were found to be normal on inspection by experienced neuroradiologists. In addition, quantitative analysis revealed normal hippocampal volumes normalized to intracranial volume, no asymmetry, and normal hippocampal T_2 values in all patients.

PET image analysis

[^{11}C]FMZ-V_d images were analysed using SPM99 (Wellcome Department of Imaging Neuroscience, London, UK) implemented in Matlab (Mathworks, Sherborn, MA, USA). The images were volumetrically normalized to a symmetrical reference FMZ-V_d template, created in our unit, that occupies the same space as the SPM99 MRI templates. The normalization procedure involves a linear 3D transformation and uses a set of smooth basis functions that allow for normalization at a finer anatomical scale (Ashburner and Friston, 1999). Images were smoothed using a 12 × 12 × 12 mm FWHM isotropic Gaussian kernel as a final preprocessing step. This spatial filter accommodates inter-individual anatomical variability and improves the sensitivity of the statistical analysis (Friston *et al*., 1991). Each subject's MRI scan was co-registered with his or her FMZ-V_d image (Woods *et al*., 1993; Ashburner and Friston, 1997) and then transformed into standard space using the transformation matrix derived from the spatial normalization of that individual's FMZ-V_d image.

Statistical analysis

Significant differences between patients and control subjects were estimated according to the general linear model at each and every voxel of the normalized and smoothed images (Friston *et al*., 1995*b*). Parametric images of FMZ-V_d were interrogated with SPM99 implemented in Matlab5 (Mathworks). Statistical parametric maps are 3D projections of statistical functions that are used to characterize significant regional differences in imaging data. We have described the use of SPM in [^{11}C]FMZ PET studies of patients with unilateral hippocampal sclerosis (Koepp *et al*., 1996), in patients with malformations of cortical development (Richardson *et al*., 1996) and in patients with TLE and normal MRI (Koepp *et al*., 2000). SPM99 combines the general linear model to create the statistical map and random field theory to make statistical inferences about regional effects (Friston *et al*., 1995*b*; Worsley *et al*., 1996).

Individual patients were compared with the 21 normal control subjects using a design matrix designating global cerebral FMZ-V_d differences as a confounding covariate (Friston *et al*., 1990). For the purposes of between-group statistical analysis, the [^{11}C]FMZ-V_d images of the six patients with right-sided TLE were reversed before spatial manipulation so that the focus was on the same (left) side in all patients. The three patients with bilateral foci (Table 1) were not included in the group analyses. Linear contrasts were used to test the hypotheses for specific focal effects. The resulting set of voxel values for each contrast constituted a statistical parametric map of the t statistic (SPM$\{t\}$). The SPM$\{t\}$ were thresholded at $P = 0.001$ uncorrected. The significance of foci of relative FMZ-V_d changes is estimated using random field theory, correcting for multiple comparisons using the number of resolution elements (resels) in the

Table 1 *Clinical, EEG and imaging data in 18 patients with refractory TLE and normal MRI*

Patient	Age (years)/ sex	Handed-ness	Onset of epilepsy (years)	Duration (years)	CPS/yr	Interval last CPS to PET (days)	Medication	EEG (inter-ictal)	EEG (ictal)	Focus*	FMZ–PET: temporal increases	FMZ–PET: temporal decreases	FMZ–PET: extratemporal abnormalities (↑/↓)
1	38/M	L	27	11	200	2	LTG	L > R temp	L temp	L	Ipsilat TLWM: *Z*3.48 *k*497 (–32/–12/–16)	Ipsilat GTS/GTM: *Z*5.04 *k*443 *P*0.002 (–52/–34/–2) and *Z*3.97 *k*240 *P*0.029 (–52/6/–22)	↓ ipsilat G frontalis medius: *Z*3.95 *k*291 *P*0.013 (–46/52/–8)
2	46/F	R	12	34	4	13	LTG/PHT	L > R temp	N/A	L	None	None	None
3	48/F	R	43	5	125	7	LTG	Bil temp	L temp	L	Bil TLWM: R *Z*4.06 *k*1185 (42/–8/24), L *Z*3.06 *k*315 (–36/–14/–22)	None	↑ ipsilat G frontalis medialis: *Z*4.31 *k*216 *P*0.041 (–6/54/0)
4	60/M	R	42	18	26	30	CBZ	L > R temp	N/A	L	Contralat TLWM: *Z*4.38 *k*4482 (36/6/–8); contralat posterior temp: *Z*3.95 *k*268 *P*0.019 (58/–38/–8)	None	None
5	47/F	R	15	32	1270	1	CBZ/PHT	R >> L temp	N/A	R	Bil TLWM: R *Z*4.45 *k*1854 (42/–12/–22), L *Z*4.04 *k*1601 (–38/–40/0)	None	None
6	24/M	R	10	14	50	10	LTG/PHT	Bi(fronto) temp indep L > R	N/A	Bil	None	R HC: *Z*2.74 *k*22 (24/–12/–24)	None
7	27/F	R	7	20	100	1	CBZ/LTG	Bil temp	4 R (fronto)-temp depth: 5 L HC, 4 R HC	Bil	None	Bil HC & bil amyg: L *Z*3.51 *k*173 (–18/–8/–22), R *Z*3.05 *k*241 (22/–10/–24)	None
8**	17/F	R	13	4	220	3	TPM/PHT	L temp	L (fronto)-temp	L	None	Ipsilat HC & amyg: *Z*3.71 *k*173 (–18/–4/–24)	None
9	64/M	R	54	10	72	6	None	L temp	N/A	L	None	None	↑ bil orbitofrontal WM and GM: L Z4.74 *k*257 *P*0.019 (–10/52/–2), R Z4.49 *k*232 *P*0.028 (28/48/–6)
10	35/M	R	16	19	8	1	LTG/PHT	L >> R temp	N/A	L	Bil TLWM: R *Z*5.47 *k*15752 (42/–10/–24), L *Z*3.88 *k*476 (–40/0/–28)	Ipsilat HC: *Z*2.88 *k*26 (–16/–10/–22)	↑ bilat WM inferolat of posterior temp horn: R *Z*5.05 *k*223 *P*0.037 (38/–44/–2), L *Z*4.69 *k*301 *P*0.012 (–34/–70/–4), bil FL WM: L *Z*4.84 *k*223 *P*0.037 (–28/30/18), R *Z*4.23 *k*599 *P*<0.001 (34/32/18), contralat frontal pole: *Z*4.28 *k*958 *P*<0.001 (26/68/–8)

Table 1 *Continued*

Patient	Age (years)/ sex	Handed-ness	Onset of epilepsy (years)	Duration (years)	CPS/yr	Interval last CPS to PET (days)	Medication	EEG (inter-ictal)	EEG (ictal)	Focus*	FMZ–PET: temporal increases	FMZ–PET: temporal decreases	FMZ–PET: extratemporal abnormalities (↑/↓)
11	28/F	R	17	11	30	8	TPM/GVG	L temp	L temp	L	Ipsilat TLWM: *Z*2.53 *k*14 (–38/–18/–10)	Ipsilat HC: *Z*2.89 *k*41 (–20/–10/–22)	None
12	30/F	R	22	8	24	21	CBZ/LTG	R temp	N/A	R	Ipsilat posterior TLWM: *Z*4.04 *k*292 (38/–46/4)	None	None
13	36/F	R	15	21	208	1	VPA/LTG	Bil indep R > L	Non localizing	Bil	L TLWM: *Z*4.18 *k*1477 (–36/–30/–12)	None	None
14	29/F	R	14	15	26	2	CBZ/LTG	L temp	L temp	L	None	None	None
15**	26/M	R	20	6	52	14	PHT/TPM/ GBP	R >> L temp	Subdural grid: R temp	R	Bil TLWM: L *Z*4.18 *k*841 (–32/–18/–34), R *Z*3.79 *k*286 (50/–14/–26)	Ipsi GTM: *Z*5.29 *k*232 *P*0.032 (70/–16/–14)	None
16	55/M	R	54	1	24	30	LTG	R temp	R temp	R	Ipsilat TLWM: *Z*3.41 *k*755 (56/–10/–24)	None	↑ ipsilat FLWM: *Z*5.35 *k*264 *P*0.02 (34/36/–14)
17**	46/F	R	26	20	72	4	GVG/LTG	R temp	R temp	R	None	Bil HC, ipsilat amyg: R *Z*3.70 *k*329 (22/–8/–22), L *Z*3.35 *k*57 (–16/–10/–22)	None
18**	42/F	R	32	10	120	3	PHT/VPA	R temp	R hemisphere non-localizing	R	Contralat TL WM: *Z*3.30 *k*149 (–34/–12/–16)	None	None

F = female, M = male, CPS = complex partial seizures, EEG = electroencephalography, N/A = not available, HC = hippocampus, LTG = lamotrigine, PHT = phenytoin, CBZ = carbamazepine, TPM = topiramate, GVG = vigabatrin, VPA = valproic acid, GBP = gabapentin, Bil = bilateral, L = left, R = right, contralat = contralateral, ipsila = ipsilat = ipsilateral, temp = temporal, amyg = amygdala, GM = grey matter, WM = white matter, TLWM = temporal lobe white matter, G = gyrus temporalis superior, GTM = gyrus temporalis medius, FL = frontal lobe, *Z* = *Z*-score compared with 21 controls, *k* = number of voxels in cluster. Coordinates in brackets are MNI coordinates, referring to our symmetrical FMZ template which is in register with the MNI/ICBM152 T1 template as supplied with SPM99. *Focus determination was based on comprehensive assessment including seizure semiology, interictal and ictal Video-EEG findings where available as well as detailed neuropsychological assessment. **Patient underwent operation; histopathology available (see text).

statistical image (Worsley *et al.*, 1992, 1996). This looks at the probability that the observed cluster of voxels could have occurred by chance, given its extent and peak height. The threshold chosen for the corrected *P* values of the extramesial clusters was $P < 0.05$. As the hippocampus, amygdala and temporal lobe white matter are small structures, below twice the FWHM of our scanner resolution, FMZ-V_d differences in these regions of special *a priori* interest were regarded as significant if the value of the *t* statistic, transformed to the unit normal distribution, exceeded a *Z*-score of >2.5, as in our previous studies (Koepp *et al.*, 1997*a*, *b*, 2000; Hammers *et al.*, 2001*a*). Age, gender, age at onset of epilepsy, duration of epilepsy, frequency of seizures, time between scan and last seizure and hippocampal volume were defined as covariates of interest and tested separately for their effect on FMZ-V_d.

The aim was to localize abnormalities of FMZ-V_d in individual patients compared with the control group and in the control group compared with the patient groups, in both grey and white matter. In SPM analyses the white matter, as a region of relatively low signal, is usually excluded by thresholding. This is done to include all areas of high signal while restricting the number of multiple comparisons by exclusion of areas that are not of interest in blood flow studies. To specifically include the entire white matter in the statistical analysis of all subjects, we therefore created an anatomical mask in template space, encompassing the grey matter in the cortex, the basal ganglia and the white matter.

In order to demonstrate the effect size, quantitative region-of-interest analyses were performed on non-normalized parametric images in the ipsilateral TLWM. An average of 2235 mm^3 was sampled with circular regions of interest, using Analyze AVW software (Robb and Hanson, 1991) in all 15 patients with a unilateral focus, and in corresponding areas in all 21 controls.

Results

Controls

Hippocampus, amygdala and TLWM

When individual control subjects were compared against the remaining 20 controls, none had FMZ-V_d abnormalities in the white matter, hippocampus or amygdala.

Extramesial structures

One individual had an increase in the anterior pallidum [$Z = 4.67$, k (number of voxels in cluster) = 390, $P = 0.003$] and another had increases in FMZ-V_d, localized to the left middle frontal gyrus ($Z = 4.30$, $k = 288$, $P = 0.011$) and the right orbitofrontal gyri ($Z = 4.25$, $k = 278$, $P = 0.013$).

Given the chosen thresholds and the number of comparisons resulting from 21 controls and two contrasts, two positive results would be predicted by chance.

Individual patients (Table 1)

Hippocampus and amygdala

Six patients had abnormally low FMZ-V_d in the hippocampus. In three of them (Patients 8, 10 and 11) the decrease was ipsilateral to the EEG focus; one of these patients (Patient 10) had additional extramesial increases and one (Patient 11) had an additional TLWM increase (see below). Two others (Patients 7 and 17) had bilateral decreases and the sixth (Patient 6) had a unilateral decrease but bilateral EEG abnormalities. The decreases extended into the amygdala in Patients 8 (Fig. 1), 7 and 17. No increases in hippocampal or amygdala FMZ-V_d were observed.

Temporal lobe white matter

Eleven of the 18 patients had FMZ-V_d increases in the TLWM. In four patients they were ipsilateral, in two contralateral, in four bilateral and in one unilateral with bilateral EEG changes. Of the four patients with ipsilateral TLWM increases (Patients 1, 11, 12 and 16), three had additional abnormalities, an ipsilateral hippocampal decrease in one (Patient 11), multiple neocortical decreases in one (Patient 1) and an ipsilateral frontal white matter increase in another (Patient 16). Of the two patients with contralateral TLWM increases (Patients 4 and 18), one (Patient 4) also had a contralateral temporal neocortical increase. Of the four patients with bilateral TLWM increases (Patients 3, 5, 10 and 15) (Fig. 2), three had additional abnormalities: a contralateral frontal increase in one (Patient 3), an ipsilateral temporal neocortical decrease in another (Patient 15) (Fig. 3) and multiple white matter increases in one (Patient 10; see below).

Extramesial structures

Seven patients showed abnormalities outside the mesial temporal structures. Only one patient (Patient 9) had extramesial abnormalities only (increases in the orbitofrontal white and grey matter bilaterally); the other six had extramesial abnormalities in addition to their temporal lobe changes described above. Extramesial decreases were found in two patients: Patient 15 (Fig. 3) had a single temporal neocortical decrease and bilateral TLWM increases; Patient 1 had decreases in the ipsilateral temporal neocortex and ipsilateral frontal lobe (FL) in addition to ipsilateral TLWM increases. Extramesial increases were found in five patients. Three had one extramesial increase only: Patient 3 in the ipsilateral FL (in addition to bilateral TLWM increases), Patient 4 in the contralateral posterior TL (in addition to a contralateral TLWM increase) and Patient 16 in the ipsilateral FL white matter (in addition to the ipsilateral TLWM increase). Two had multiple extramesial increases. Patient 9 had bifrontal increases. Patient 10 had multiple white matter increases inferolaterally of both posterior temporal horns and

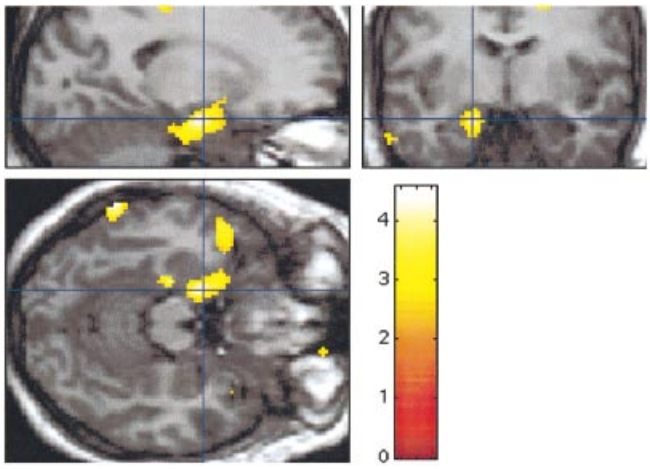

Fig. 1 Example of a patient (Patient 8) with decreased FMZ-V_d in the ipsilateral hippocampus extending into the amygdala. Colour scale: *Z* score (maximum $Z = 3.71$). Statistical results are overlaid onto the patient's co-registered MRI. Only the mesial temporal decrease, highlighted with a cross-hair, is significant. The left side of the coronal image and the upper part of the transverse image correspond to the left side of the brain.

in both FLs, in addition to bilateral TLWM increases and an ipsilateral hippocampal decrease.

Between-group analyses

Hippocampus/amygdala

There was a decrease in FMZ-V_d in the ipsilateral hippocampus in the patient group, extending into the amygdala ($Z = 3.01$), as well as in the contralateral hippocampus ($Z = 2.56$) (Fig. 4).

Temporal lobe white matter

The patient group showed ipsilateral ($Z = 3.71$) and contralateral (two clusters, $Z = 3.11$ and $Z = 2.79$) increases in FMZ-V_d (Fig. 4).

In order to demonstrate the magnitude of the effect, quantitative region-of-interest analyses were performed on non-normalized parametric images. The ipsilateral TLWM was sampled in all 15 patients with a unilateral focus and corresponding areas were sampled in all 21 controls. These showed an average increase in FMZ-V_d of 16% in ipsilateral TLWM in the patients, which was highly significant (two-tailed *t* test, $P < 0.007$).

Extramesial structures

We found increased FMZ-V_d in the ipsilateral frontal lobe white matter (FLWM) between the superior and medial frontal gyrus ($Z = 3.80$, $k = 293$, $P < 0.025$), with similar changes contralaterally ($Z = 4.87$, $k = 510$, $P < 0.0004$). There were no decreases outside the mesial temporal lobe.

Correlations with clinical data

There were no correlations anywhere in the brain between FMZ-V_d and age, gender, age at onset of epilepsy, duration of epilepsy, frequency of seizures, time between scan and last seizure, or hippocampal volume.

Surgery and histological results

So far, four patients have had surgery. One patient (Patient 15), with a marked unilateral temporal neocortical decrease in FMZ-V_d in addition to bilateral TLWM increases, has had a focal cortical resection. Histology showed a small malformative lesion with some features similar to Taylor-type focal cortical dysplasia (Taylor *et al*., 1971). There were dysplastic neurones in the cortex and gliosis. The demarcation between the grey and white matter was poorly defined. There were abnormal, large neurones present in the white matter, but only a small amount of white matter was resected and neuronal density could not be quantified. The patient remains seizure-free 25 months after the operation.

Three patients (Patients 8, 17 and 18) underwent modified anterior temporal lobe resections. One patient (Patient 8), with a left hippocampal decrease in FMZ-V_d extending into the amygdala, had a left anterior temporal lobe resection including the amygdala and hippocampus at another centre. Unfortunately, tissue was not preserved for detailed histological analysis and the hippocampal formation could not be identified in the resection specimen. The resected cortex showed moderate subpial and white matter gliosis. The patient remains seizure-free 26 months after the operation but has suffered a significant decline in verbal memory. Patient 17 had an ipsilateral (right) decrease in FMZ binding in the hippocampus and amygdala. A decrease in contralateral hippocampal FMZ binding was less marked in terms of both *Z* score and spatial extent. Pathology showed amygdala gliosis (Fig. 5C and D) and mild end folium sclerosis (Fig. 5E). Immunohistochemistry with neuronal nuclear antigen (NeuN) and quantification showed low neuronal density in the TLWM (Fig. 5B) (1010/mm^3; control mean 1660 $\pm$ 772 mm^3 (Thom *et al*., 2001)). The patient has been seizure-free for 4 months after the operation but recently had a single seizure within two weeks of starting fluoxetine. Patient 18 had no ipsilateral (right) abnormalities on FMZ PET but contralateral increases in FMZ binding in TLWM. On pathology, the right hippocampus was not fully represented, but parts of CA1, CA4 and the subiculum were available. There was mild gliosis but no evidence to support classical hippocampal sclerosis. TLWM neuronal density on quantitative immunohistochemistry with NeuN was moderately high (Fig. 5A) at 2368/mm^3. The patient currently remains seizure-free 4 months after the operation.

One patient (Patient 7) with bilateral decreases in hippocampal FMZ-V_d, more marked on the left, has been evaluated with bilateral hippocampal depth electrodes. Nine

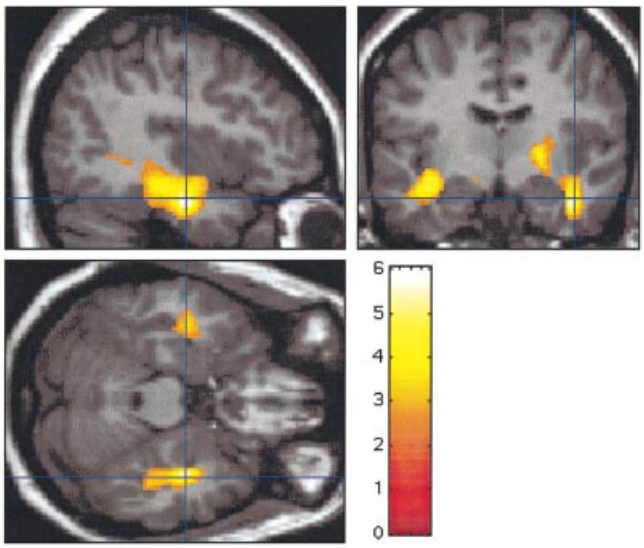

Fig. 2 Example of a patient (Patient 5) with increased FMZ-V_d in the TLWM bilaterally. Colour scale: Z score (maximum $Z = 4.45$). Statistical results are overlaid onto the patient's co-registered MRI. Only the ipsilateral TLWM increase (highlighted with a cross-hair) and the contralateral TLWM increase are significant. The left side of the coronal image and the upper part of the transverse image correspond to the left side of the brain.

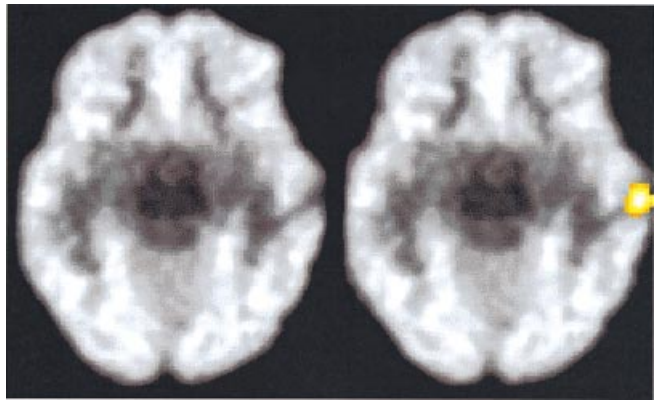

Fig. 3 Isolated ipsilateral neocortical decrease in FMZ-V_d in Patient 15. Pathology showed a small malformative lesion similar to Taylor-type focal cortical dysplasia. Statistical results (maximum $Z = 5.29$) are shown overlaid onto the patient's normalized FMZ-V_d image on the left. The right of the image shows that this decrease is visible even before statistical analysis. Left side of the images corresponds to the left side of the brain.

seizures were recorded; five started within the right and four within the left hippocampus.

Discussion

Patients with TLE and normal high-resolution MRI represent a challenge in epilepsy surgery referral centres. This is the largest study of such a group so far and the first to examine white matter changes in FMZ-V_d explicitly in these patients. The main novel finding is the high proportion (61%) of patients with increased FMZ binding in the white matter.

In total, we found abnormalities in 16 out of 18 patients with TLE and normal high-resolution MRI, which included volumetric hippocampal studies and hippocampal T_2 quantitation, confirming that [^{11}C]FMZ PET detects functional abnormalities over and above the structural abnormalities revealed by optimal MRI (Koepp *et al*., 1997*b*, 2000). Moreover, in this study the abnormalities found were surgically relevant in the six patients with unilateral or asymmetrical bilateral decreases in hippocampal FMZ-V_d and in the one patient with a single temporal neocortical decrease.

Methodological considerations and comparison with previous findings

SPM is a voxel-based approach that examines the entire 3D brain volume data set and has been validated for the interpretation of ligand PET scans in epilepsy (Koepp *et al.*, 1996, 2000; Richardson *et al.*, 1996, 1997, 1998). While SPM localizes receptor binding abnormalities, it cannot differentiate between structural and functional abnormalities. The effect of anatomical abnormalities can be accounted for using both voxel-based (Richardson *et al*., 1997) and region-based (Koepp *et al*., 1997*a*, 2000; Hammers *et al*., 2001*a*) analyses. In this study, we only included patients whose MRI was normal on inspection and in whom quantitative analysis of the hippocampi, including volumetry and T_2 mapping, was entirely normal. In this situation, SPM is superior to region-based analyses as the entire brain volume can be studied and no assumptions about the number, localization and extent of abnormalities need to be made. Interpolation and smoothing necessarily decrease the spatial resolution of the resulting statistical map to ~13 mm FWHM. In contrast, the final spatial resolution of region-based analyses depends on the number and size of regions chosen (typically 10–50 for a given brain imaging data set). SPM examines the data at our level of smoothing with ~500 independent comparisons and without *a priori* hypotheses about the exact localization of neocortical abnormalities.

SPM does, however, need rigorous correction for the multiple comparisons made in order to prevent spurious false positives. If such a correction is applied to the entire volume, mesial temporal abnormalities, which are small in extent, may remain undetected. For mesial temporal structures (hippocampus and amygdala) and temporal white matter, we had *a priori* hypotheses. Within this defined small search volume (approximately four resolution elements), we did not correct for the spatial extent of the clusters of abnormal FMZ binding, but only for height, as in our previous studies (Koepp *et al*., 1997*a*, *b*, 2000; Hammers *et al*., 2001*a*). The validity of this approach was tested by investigating each control against the remaining 20 controls, and no mesial temporal false positives were detected. This rigorous exclusion of detection of artefactual increases or decreases amounts to a random effect analysis on our normal material.

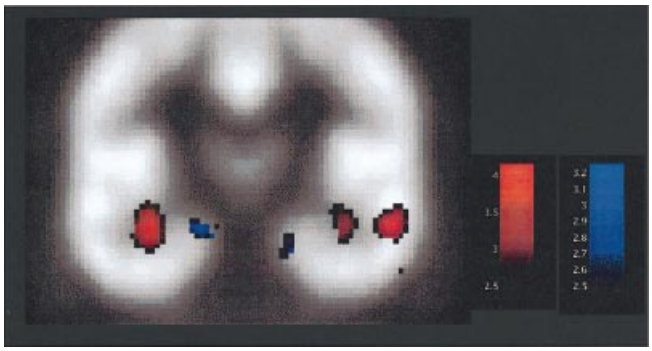

Fig. 4 Group comparison. (*Red*) Patients show ipsilateral ($Z = 3.71$, left of the image) and contralateral increases [two clusters, $Z = 3.11$ and $Z = 2.79$ (not shown)] in FMZ-V_d in the TLWM. (*Blue*) Patients show decreases in FMZ-V_d in the ipsilateral hippocampus ($Z = 3.01$) extending into the amygdala, and in the contralateral hippocampus ($Z = 2.56$). Statistical results are overlaid onto the FMZ template used for normalization. Colour bars indicate *t* scores.

In a previous study, we compared 10 different patients with normal quantitative MRI whose scans were acquired in temporal lobe orientation with 13 different controls with MRI acquired in temporal lobe orientation, using both an earlier version of SPM (SPM96) and partial volume effect correction (Koepp *et al*., 2000). Although FMZ-V_d abnormalities were shown in eight of 10 patients, unilateral decreases were concordant with EEG data in only two, and most TLWM was excluded from the analysis by the use of standard thresholding methods.

The larger control group in this study makes the analysis more sensitive. Furthermore, the process of spatial normalization has been much improved in SPM99 (Ashburner and Friston, 1997, 1999). Better registration, particularly of the small mesial temporal structures, contributes to increased sensitivity and specificity.

We previously found a strong correlation ($r > 0.8$, $P < 0.001$) between preoperative white matter FMZ-V_d in both temporal lobes and the white matter neurone number determined in the resected ipsilateral specimen of patients with hippocampal sclerosis (Hammers *et al*., 2001*a*). Increased TLWM neurone number is a hallmark of microdysgenesis. In this study, we investigated the hypothesis that microdysgenesis, manifesting itself as increased TLWM FMZ-V_d, could underlie some of the cases of TLE and normal MRI. SPM was originally devised for the study of grey matter, and thresholding normally excludes white matter from the analysis. Lowering this blanket threshold to include white matter signal gives inconsistent results due to the interindividual variability in global binding and increases the number of voxels included in the analysis, thereby accentuating the multiple comparisons problem. We therefore created an anatomical mask in template space, encompassing the grey matter in the cortex and basal ganglia as well as the central white matter. This enabled us to study explicitly, for the first time, white matter changes while restricting the number of voxels inspected. There is a theoretical concern that the error distribution could become positively skewed in areas of low binding due to the non-negativity constraint. The actual values derived from region-of-interest studies, however, indicate that mean values were more than 10 standard deviations away from zero in the TLWM, and the error distribution can therefore be approximated by parametric measures of variability.

Neurobiological considerations

There is now extensive evidence that decreased FMZ binding can localize the epileptogenic focus both in mesial TLE and in neocortical epilepsy (Savic *et al*., 1988, 1993, 1995; Henry *et al*., 1993; Koepp *et al*., 1996, 1997*b*; Szelies *et al*., 1996; Ryvlin *et al*., 1998; Muzik *et al*., 2000).

In earlier studies that included both patients with hippocampal sclerosis and patients with normal MRI, there was a clear negative correlation between hippocampal volume and FMZ binding (Henry *et al*., 1993; Lamusuo *et al*., 2000). Hippocampal FMZ binding is, however, reduced over and above volume loss in hippocampal sclerosis (Henry *et al*., 1993; Koepp *et al*., 1997*a*, *b*; Hammers *et al*., 2001*a*), indicating functional abnormalities over and above evident structural abnormalities. Our results suggest that the same is true for TLE with normal quantitative MRI: both the group of patients and six out of 18 individual patients showed a significant decrease in hippocampal FMZ-V_d despite normal quantitative MRI. Moreover, there was no correlation between hippocampal volume and hippocampal FMZ-V_d, further indicating that our results were not due to atrophy or partial volume effect.

FMZ binds with high affinity to the benzodiazepine binding site of $GABA_A$ receptors containing α_1, α_2, α_3 and α_5 subunits, and therefore our study can only look at the sum of effects of changes in these subunits. TLE is associated not only with changes in $GABA_A$ receptor number but also with differential changes in subunit composition (Brooks-Kayal *et al*., 1998; Sperk *et al*., 1998; Loup *et al*., 2000) that may precede the development of epilepsy in rats (Brooks-Kayal *et al*., 1998). With the development of subunit-specific tracers, it may be possible in the future to study epileptogenesis *in vivo*.

We found increases in FMZ-V_d in the TLWM in 11 out of 18 patients with TLE and normal MRI. We suggest that these are due to microdysgenesis, i.e. an increased number of neurones in the white matter. There is a large body of direct and indirect evidence to support this claim. (i) We have previously shown a strong correlation between TLWM FMZ-V_d and histologically determined neurone number in the white matter in patients with hippocampal sclerosis (Hammers *et al*., 2001*a*). (ii) In the three patients (Patients 15, 17 and 18) in the present series for whom TLWM was available for pathology, the prediction about the presence or absence of heterotopic neurones based on FMZ PET was confirmed and was quantified immunohistochemically with

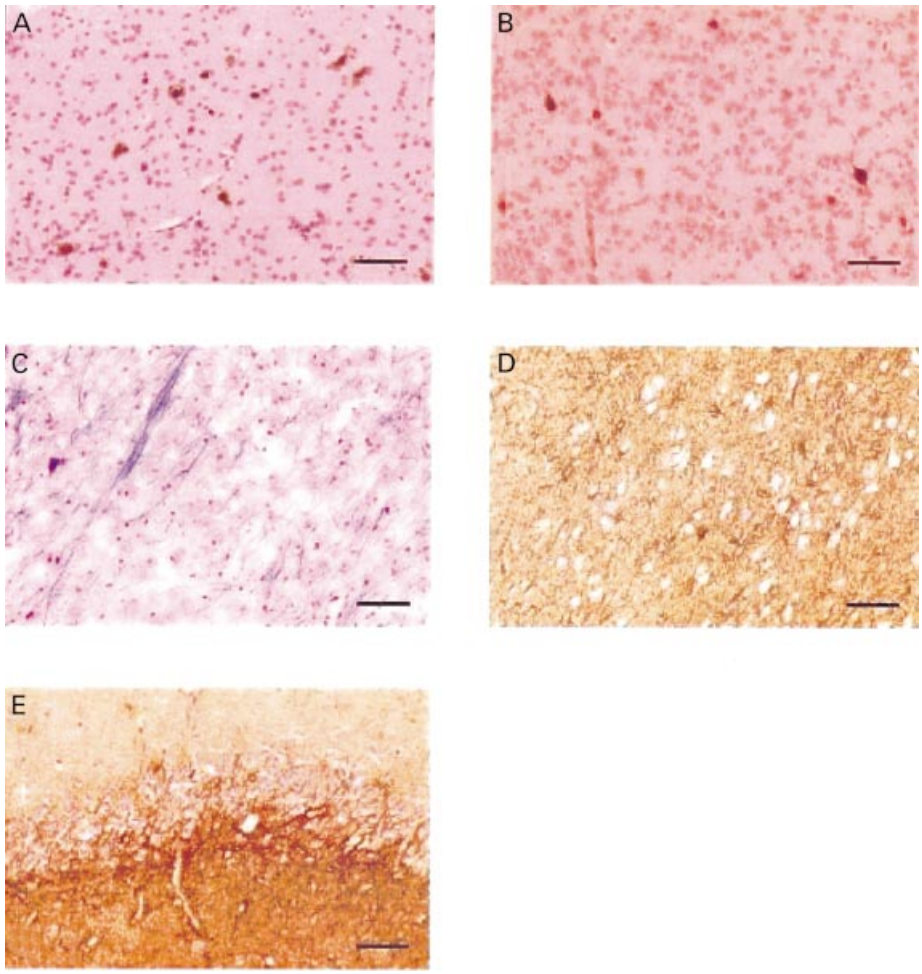

Fig. 5 (**A** and **B**) White matter neurones labelled with neuronal marker NeuN in Patient 18 (**A**) and Patient 17 (**B**), which demonstrated a lower number of both large and small neurones in a similar size field in **B** than **A**. (**C**) Luxol fast blue-stained section of the amygdala resection from Patient 17 shows some preservation of neurones, but marked diffuse gliosis is seen in the adjacent section immunostained for GFAP (glial fibrillary acidic protein) (**D**). (**E**) GFAP immunostaining in Patient 17 also demonstrated marked gliosis in the end folium (lower half of the field) extending into the granule cell layer and compatible with the diagnosis of end folium sclerosis. Bars = 50 μm.

NeuN in two cases (Patients 17 and 18), directly validating our results. (iii) Increases in FMZ-V_d were frequently seen in malformations of cortical development (Richardson *et al.*, 1996, 1997) but not in acquired lesions (Richardson *et al.*, 1998). (iv) Histopathological studies of malformations of cortical development in humans have frequently shown increased white matter neurone numbers (Burdette *et al.*, 1995; Battaglia *et al.*, 1996; Spreafico *et al.*, 1998; Hannan *et al.*, 1999).

Theoretically, an increase in TLWM FMZ binding could be due to an apparent, relative rather than absolute increase in heterotopic neuronal density due to atrophy. We do not believe this can explain our results for the following reasons. (i) After the electroclinical diagnosis of TLE had been made, all MRIs were reviewed carefully with particular attention to the temporal lobes. No abnormality was found on inspection by experienced neuroradiologists or in either the quantitative volumetric studies or the T_2 quantification studies of the hippocampi. The MRIs can therefore be regarded as normal by best current standards (Commission on Neuroimaging of the International League Against Epilepsy, 1997). (ii) Even minimal temporal lobe atrophy will be detected by SPM as a widespread decrease in FMZ binding along the border of the temporal neocortex (Hammers *et al.*, 2001*a*), and this was not seen in this study. (iii) Neuronal density in the white matter does not correlate with the 3D volume of the white matter (Bothwell *et al.*, 2001) or white matter gliosis (Kasper *et al.*, 1999; Thom *et al.*, 2001).

FMZ–PET is well suited to reflect abnormal neuronal density in white matter *in vivo*. Most neurones express $GABA_A$ receptors and FMZ can, therefore, be regarded to a certain extent as a neuronal marker. Whereas clusters of heterotopic neurones need to be at least 1 mm^3 in size to be evident on MRI, the signal-to-noise ratio for heterotopic neurones in the white matter is very high for PET. The highly specific nature of FMZ binding makes it very improbable that

these findings are functional in nature, in contrast to some abnormalities in grey matter FMZ binding (Ryvlin *et al*., 1999) or metabolic ([^{18}F]fluorodeoxyglucose–PET) imaging.

Heterotopic white matter neurones can contribute to epileptogenesis by providing additional or abnormal circuitry. This has been shown experimentally for heterotopic CA1 neurones in the rat model of methylazoxymethanol-induced cortical malformations (Chevassus-au-Louis *et al*., 1998). The finding of heterotopic white matter neurones in TLE with normal MRI can, therefore, be a reasonable explanation for the pathogenesis of epileptic circuits in the face of normal structural imaging studies. The relevance of our findings for TLE is further underlined by the fact that 11 out of 18 patients but 0 out of 21 controls showed TLWM increases (χ^2 test, $P < 0.0001$).

Taken as a group, the patients showed significant increases in FMZ-V_d in the FLWM bilaterally. Widespread disturbances of cerebral structure have been demonstrated in malformations of cortical development (e.g. Richardson *et al*., 1997). The most tenable explanation for these increases in FMZ-V_d in the white matter is again the presence of heterotopic white matter neurones. We do not, however, have histological material to prove this. Moreover, in the individual analysis, FLWM increases in FMZ-V_d at a location closely related to that of the group finding were found in only one patient (Patient 10), who had very widespread white matter increases. It would be reasonable to assume that a diffuse disturbance of migration can manifest itself principally in the TLWM but have some smaller effect elsewhere. Frontal lobe white matter contains approximately six times fewer neurones in controls than TLWM (Rojiani *et al*., 1996), and our finding is compatible with a small effect size which reaches significance in SPM due to its large spatial extent and the large number of subjects studied.

Clinical considerations

Patients with normal or non-diagnostic MRI and medically refractory TLE are an important and difficult subgroup of patients who undergo investigations for epilepsy surgery. Accordingly, there have been various studies using FMZ–PET centred on or including 'MRI-negative' TLE patients (Henry *et al*., 1993; Savic *et al*., 1993; Szelies *et al*., 1996; Debets *et al*., 1997; Ryvlin *et al*., 1998; Koepp *et al*., 2000; Lamusuo *et al*., 2000). In most earlier studies, however, MRI was only assessed qualitatively for signs of hippocampal sclerosis, and quantitative hippocampal MRI data were only available in three studies (Ryvlin *et al*., 1998; Koepp *et al*., 2000; Lamusuo *et al*., 2000). Also, most of the earlier studies relied on measures of asymmetry for both hippocampal volumes and FMZ binding and could not therefore detect bilateral abnormalities.

In our series, amongst other findings, there were patients with hippocampal decreases in FMZ binding, most likely representing hippocampal damage; subjects with TLWM increases, most likely representing microdysgenesis; and subjects with both. This heterogeneity is hardly surprising as the group of MRI-negative patients will include patients with any pathology not detectable with current optimal MRI. Both hippocampal decreases and white matter increases in FMZ binding were detected in the group comparison despite subject heterogeneity. We therefore believe that both are common mechanisms in MRI-negative TLE.

Our decisions on which patients to include were based on the electroclinical diagnosis of TLE. Ictal video–EEG was not obtained in seven patients, but we do not believe that overemphasis should be placed on ictal EEG in this situation. A case in point is Patient 7 (Table 1), who would have been misclassified as having right TLE on the basis of four ictal surface EEG recordings but was correctly classified as having bitemporal foci on the basis of the remainder of the electroclinical data. FMZ–PET subsequently showed bilateral mesial temporal decreases in FMZ-V_d, and depth recordings confirmed the bilateral independent onset of seizures. In suspected bitemporal epilepsy, FMZ–PET may therefore help to confirm the bilateral origin (Ryvlin *et al*., 1998).

In our series, three patients (Patients 8, 17 and 18) have undergone modified anterior temporal lobe resections to date. Two (Patients 8 and 18) are currently seizure-free 26 and 4 months after the operation, respectively, and one (Patient 17) has had a single seizure within 2 weeks of starting fluoxetine therapy after 4 months without seizures, compared with six seizures per month before the operation. Despite the short follow-up in the last two cases, this suggests that the decrease in hippocampal FMZ-V_d detected by SPM indeed reflected the epileptic focus.

Two of the operated cases (Patients 8 and 17) had ipsilateral hippocampal decreases in FMZ-V_d, accompanied by amygdala decreases in the case of Patient 17. For the patient operated in our centre (Patient 17), pathology was available and showed amygdala sclerosis as well as mild hippocampal end folium sclerosis, confirming that end folium sclerosis and amygdala sclerosis may be associated with decreases in FMZ-V_d, even if high-resolution MRI is unremarkable.

In two of the operated cases (Patients 17 and 18), sufficient amounts of TLWM were available to quantify TLWM neuronal density immunohistochemically with NeuN, a specific neuronal marker, as described recently (Thom *et al*., 2001). In Patient 17, no TLWM increases were detected on FMZ PET, and immunohistochemistry confirmed low neuronal densities (1010/mm^3). In Patient 18, contralateral but not ipsilateral increases in TLWM FMZ binding were seen. Immunohistochemistry showed ipsilateral neuronal densities in the high normal range (2368/mm^3). Ipsilateral high normal neuronal densities are compatible with the concept of microdysgenesis as a diffuse process, while the fact that they were not significantly elevated corroborates our PET finding.

Another patient (Patient 15) with a small area of significant FMZ-V_d decrease in the ipsilateral temporal neocortex and bilateral TLWM FMZ-V_d increases was operated upon and

found to have a malformative lesion similar to a Taylor-type focal cortical dysplasia (Taylor *et al*., 1971). Pathology showed abnormal white matter neurones, although the amount of resected white matter was not sufficient to quantify them. He remains seizure-free 25 months after the operation. This case confirms that focal cortical malformations may be associated with decreases in FMZ-V_d, even if MRI is unremarkable, and represents further evidence for the pathological equivalent of increases in FMZ-V_d detected *in vivo*. Furthermore, besides the confirmation that malformations may indeed be associated with increases in FMZ-V_d in white matter, in this single case, at least, bilateral white matter changes did not seem to affect the prognosis adversely after surgery in the limited duration of available follow-up.

This would be in keeping with an early study of temporal lobe surgery, before MRI diagnosis of hippocampal sclerosis *in vivo* became widely available (Hardiman *et al*., 1988). Fifty patients were treated with anterior temporal lobe resection, sparing the hippocampus and the amygdala. Severe neuronal ectopia was present in 42% of patients, and 28% showed neuronal clustering. Interestingly, both were predictive of good clinical outcome. The rate of seizure-free patients (52%) was lower than in contemporary series with removal of the hippocampus and amygdala. The study does, however, raise the intriguing possibility that, in some cases with microdysgenesis, resection of heterotopic white matter neurones may be sufficient to achieve freedom from seizures and suggests the possibility that seizures may arise from epileptogenic networks that involve white matter.

A caveat when considering patients with bilateral TLWM increases are reports of worse postoperative outcome after surgery in patients with intractable TLE (mostly found to have hippocampal sclerosis) when there were high numbers of white matter neurones (Kasper *et al*., 1999) and our own finding of a positive correlation between increased FMZ-V_d in the TLWM contralateral to the lobe resected for hippocampal sclerosis with outcome poorer than Engel class IA (Hammers *et al*., 2001*a*).

In contrast, Choi and colleagues found a better surgical outcome for hippocampal sclerosis patients with MRI-detectable TLWM changes which correlated with heterotopic neurone number (Choi *et al*., 1999). The groups were, however, defined through the MRI findings before white matter neurones were counted, and the fact that patients with more damage tend to have a better outcome (Jack *et al*., 1992) may have been a confounding factor. Finally, Thom and colleagues used immunohistochemistry and a rigorous quantitative approach with 3D cell counting methods in 31 patients with MRI-diagnosed and pathologically confirmed hippocampal sclerosis (Thom *et al*., 2001). The 17 out of 26 patients with sufficient follow-up who became seizure-free had significantly higher TLWM neuronal densities and other microdysgenetic features than the nine out of 26 who did not. As with all surgical studies, only tissue ipsilateral to the hippocampal sclerosis could be studied.

These findings need not be contradictory. It is conceivable that microdysgenesis may sometimes be due to generalized disturbances of neuronal migration or cell death. In these cases, heterotopic neurones are merely a marker of more widespread disturbance and consequently prognosis may be affected adversely (Hammers *et al*., 2001*a*). In other cases, however, when migration or cell death are disturbed only locally, surgical interruption of abnormal circuits involving heterotopic neurones (Chevassus-au-Louis *et al*., 1998) may be sufficient to achieve freedom from seizures, and in these cases microdysgenesis may indicate a better prognosis (Hardiman *et al*., 1988; Choi *et al*., 1999; Thom *et al*., 2001).

In summary, we have optimized the analysis of FMZ–PET scans by adapting SPM99 to the analysis of grey and white matter changes in TLE with normal high-resolution and quantitative MRI. We were able to increase the yield of both non-invasively detected abnormalities and surgically relevant abnormalities. Inclusion of the white matter in the analysis provides new and interesting insights into the pathophysiology of 'MRI-negative' TLE. FMZ–PET provides useful information in a significant proportion of potential surgical candidates.

Acknowledgements

We wish to thank our colleagues at the MRC Cyclotron Building (particularly Andrew Blyth, Joanne Holmes, Leonhard Schnorr and Drs Richard Banati, Peter Bloomfield, Matthew Brett, Annachiara Cagnin, Roger Gunn, Ralph Myers and Federico Turkheimer) for help in the acquisition and analysis of PET data; Professors Ley Sander, Simon Shorvon and David Fish, Drs Sanjay Sisodiya and Shelagh Smith and Catherine Scott for referring patients, Mr William Harkness for performing the surgical resections, Dr Pamela Thompson for the neuropsychological data, our colleagues at the National Society for Epilepsy for performing and transferring the MRI scans and Dr Barbara Swartz for helpful discussions. Action Research (SP 3123), the National Society for Epilepsy, the Medical Research Council and the Deutsche Forschungsgemeinschaft (Ha 3013/1–1) provided support.

References

Ashburner J, Friston K. Multimodal image coregistration and partitioning—a unified framework. Neuroimage 1997; 6: 209–17.

Ashburner J, Friston KJ. Nonlinear spatial normalization using basis functions. Hum Brain Mapp 1999; 7: 254–66.

Babb TL, Brown WJ, Pretorius J, Davenport C, Lieb JP, Crandall PH. Temporal lobe volumetric cell densities in temporal lobe epilepsy. Epilepsia 1984; 25: 729–40.

Bailey DL. 3D acquisition and reconstruction in positron emission tomography. Ann Nucl Med 1992; 6: 123–30.

Battaglia G, Arcelli P, Granata T, Selvaggio M, Andermann F, Dubeau F, et al. Neuronal migration disorders and epilepsy: a

morphological analysis of three surgically treated patients. Epilepsy Res 1996; 26: 49–58.

Berkovic SF, McIntosh AM, Kalnins RM, Jackson GD, Fabinyi GC, Brazenor GA, et al. Preoperative MRI predicts outcome of temporal lobectomy: an actuarial analysis. Neurology 1995; 45: 1358–63.

Bothwell S, Meredith GE, Phillips J, Staunton H, Doherty C, Grigorenko E, et al. Neuronal hypertrophy in the neocortex of patients with temporal lobe epilepsy. J Neurosci 2001; 21: 4789–800.

Brooks-Kayal AR, Shumate MD, Jin H, Rikhter TY, Coulter DA. Selective changes in single cell $GABA_A$ receptor subunit expression and function in temporal lobe epilepsy. Nat Med 1998; 4: 1166–72.

Burdette DE, Sakurai SY, Henry TR, Ross DA, Pennell PB, Frey KA, et al. Temporal lobe central benzodiazepine binding in unilateral mesial temporal lobe epilepsy. Neurology 1995; 45: 934–41.

Chevassus-au-Louis N, Congar P, Represa A, Ben-Ari Y, Gaiarsa J-L. Neuronal migration disorders: heterotopic neocortical neurons in CA1 provide a bridge between the hippocampus and the neocortex. Proc Natl Acad Sci USA 1998; 95: 10263–8.

Choi D, Na DG, Byun HS, Suh YL, Kim SE, Ro DW, et al. White-matter change in mesial temporal sclerosis: correlation of MRI with PET, pathology, and clinical features. Epilepsia 1999; 40: 1634–41.

Chugani HT, Shields WD, Shewmon DA, Olson DM, Phelps ME, Peacock WJ. Infantile spasms: I. PET identifies focal cortical dysgenesis in cryptogenic cases for surgical treatment. Ann Neurol 1990; 27: 406–13.

Commission on Neuroimaging of the International League Against Epilepsy. Recommendations for neuroimaging of patients with epilepsy. Epilepsia 1997; 38: 1255–6.

Cunningham VJ, Jones T. Spectral analysis of dynamic PET studies. J Cereb Blood Flow Metab 1993; 13: 15–23.

Debets RM, Sadzot B, van Isselt JW, Brekelmans GJ, Meiners LC, van Huffelen AO, et al. Is ^{11}C-flumazenil PET superior to ^{18}FDG PET and ^{123}I-iomazenil SPECT in presurgical evaluation of temporal lobe epilepsy? J Neurol Neurosurg Psychiatry 1997; 62: 141–50.

Desbiens R, Berkovic SF, Dubeau F, Andermann F, Laxer KD, Harvey S, et al. Life-threatening focal status epilepticus due to occult cortical dysplasia. Arch Neurol 1993; 50: 695–700.

Duncan JS, Bartlett P, Barker GJ. Technique for measuring hippocampal T2 relaxation time. AJNR Am J Neuroradiol 1996; 17: 1805–10.

Friston KJ, Frith CD, Liddle PF, Dolan RJ, Lammertsma AA, Frackowiak RS. The relationship between global and local changes in PET scans. J Cereb Blood Flow Metab 1990; 10: 458–66.

Friston KJ, Frith CD, Liddle PF, Frackowiak RS. Comparing functional (PET) images: the assessment of significant change. J Cereb Blood Flow Metab 1991; 11: 690–9.

Friston KJ, Ashburner J, Frith CD, Poline JB, Heather JD, Frackowiak RSJ. Spatial registration and normalization of images. Hum Brain Mapp 1995a; 3: 165–89.

Friston KJ, Holmes AP, Worsley KJ, Poline JB, Frith CD, Frackowiak RSJ. Statistical parametric maps in functional imaging: a general linear approach. Hum Brain Mapp 1995b; 2: 189–210.

Grootoonk S. Dual energy window correction for scattered photons in 3-D positron emission tomography [PhD thesis]. Guildford (UK): University of Surrey; 1995.

Hammers A, Koepp MJ, Labbé C, Brooks DJ, Thom M, Cunningham VJ, et al. Neocortical abnormalities of [^{11}C]-flumazenil PET in mesial temporal lobe epilepsy. Neurology 2001a; 56: 897–906.

Hammers A, Koepp MJ, Richardson MP, Labbé C, Brooks DJ, Cunningham VJ, et al. Central benzodiazepine receptors in malformations of cortical development. A quantitative study. Brain 2001b; 124: 1555–65.

Hammers A, Koepp MJ, Free SL, Brett M, Richardson MP, Labbé C, et al. Implementation and application of a brain template for multiple volumes of interest. Hum Brain Mapp 2002; 15: 165–74.

Hand KS, Baird VH, Van Paesschen W, Koepp MJ, Revesz T, Thom M, et al. Central benzodiazepine receptor autoradiography in hippocampal sclerosis. Br J Pharmacol 1997; 122: 358–64.

Hannan AJ, Servotte S, Katsnelson A, Sisodiya S, Blakemore C, Squier M, et al. Characterization of nodular neuronal heterotopia in children. Brain 1999; 122: 219–38.

Hardiman O, Burke T, Phillips J, Murphy S, O'Moore B, Staunton H, et al. Microdysgenesis in resected temporal neocortex: incidence and clinical significance in focal epilepsy. Neurology 1988; 38: 1041–7.

Henry TR, Frey KA, Sackellares JC, Gilman S, Koeppe RA, Brunberg JA, et al. In vivo cerebral metabolism and central benzodiazepine–receptor binding in temporal lobe epilepsy. Neurology 1993; 43: 1998–2006.

Jack CR Jr, Sharbrough FW, Cascino GD, Hirschorn KA, O'Brien PC, Marsh WR. Magnetic resonance image-based hippocampal volumetry: correlation with outcome after temporal lobectomy. Ann Neurol 1992; 31: 138–46.

Kasper BS, Stefan H, Buchfelder M, Paulus W. Temporal lobe microdysgenesis in epilepsy versus control brains. J Neuropathol Exp Neurol 1999; 58: 22–8.

Koepp MJ, Richardson MP, Brooks DJ, Poline JB, Van Paesschen W, Friston KJ, et al. Cerebral benzodiazepine receptors in hippocampal sclerosis. An objective in vivo analysis. Brain 1996; 119: 1677–87.

Koepp MJ, Labbé C, Richardson MP, Brooks DJ, Van Paesschen W, Cunningham VJ, et al. Regional hippocampal [^{11}C]flumazenil PET in temporal lobe epilepsy with unilateral and bilateral hippocampal sclerosis. Brain 1997a; 120: 1865–76.

Koepp MJ, Richardson MP, Labbé C, Brooks DJ, Cunningham VJ, Ashburner J, et al. ^{11}C-flumazenil PET, volumetric MRI, and quantitative pathology in mesial temporal lobe epilepsy. Neurology 1997b; 49: 764–73.

Koepp MJ, Hand KS, Labbé C, Richardson MP, Van Paesschen W, Baird VH, et al. In vivo [^{11}C]flumazenil-PET correlates with ex vivo [^{3}H]flumazenil autoradiography in hippocampal sclerosis. Ann Neurol 1998; 43: 618–26.

Koepp MJ, Hammers A, Labbé C, Woermann FG, Brooks DJ, Duncan JS. 11C-flumazenil PET in patients with refractory temporal lobe epilepsy and normal MRI. Neurology 2000; 54: 332–9.

Koeppe RA, Holthoff VA, Frey KA, Kilbourn MR, Kuhl DE. Compartmental analysis of [^{11}C] flumazenil kinetics for the estimation of ligand transport rate and receptor distribution using positron emission tomography. J Cereb Blood Flow Metab 1991; 11: 735–44.

Kuzniecky RI, Jackson GD. Developmental disorders. In: Engel J Jr, Pedley TA, editors. Epilepsy: a comprehensive textbook. Philadelphia: Lippincott-Raven; 1998. p. 2517–32.

Kuzniecky R, Garcia JH, Faught E, Morawetz RB. Cortical dysplasia in temporal lobe epilepsy: magnetic resonance imaging correlations. Ann Neurol 1991; 29: 293–8.

Lammertsma AA, Lassen NA, Prevett MC, Bartenstein PA, Turton DR, Luthra SK, et al. Quantification of benzodiazepine receptors in vivo using [^{11}C]flumazenil: application of the steady state principle. In: Uemura K, Lasson NA, Jones T, Kanno I, editors. Quantification of brain function. Tracer kinetic and image analysis in brain PET. Amsterdam: Elsevier Science; 1993. p. 303–11.

Lamusuo S, Pitkänen A, Jutila L, Ylinin A, Partanen K, Kälviäinen R, et al. [^{11}C]Flumazenil binding in the medial temporal lobe in patients with temporal lobe epilepsy. Correlation with hippocampal MR volumetry, T2 relaxometry, and neuropathology. Neurology 2000; 54: 2252–60.

Loup F, Wieser HG, Yonekawa Y, Aguzzi A, Fritschy JM. Selective alterations in $GABA_A$ receptor subtypes in human temporal lobe epilepsy. J Neurosci 2000; 20: 5401–19.

Maziere M, Hantraye P, Prenant C, Sastre J, Comar D. Synthesis of ethyl 8-fluoro-5,6-dihydro-5-[^{11}C]methyl-6-oxo-4H-imidazo [1,5-a][1,4]benzodiazepine-3-carboxylate (RO 15.1788–11C): a specific radioligand for the in vivo study of central benzodiazepine receptors by positron emission tomography. Int J Appl Radiat Isot 1984; 35: 973–6.

Muzik O, da Silva EA, Juhasz C, Chugani DC, Shah J, Nagy F, et al. Intracranial EEG versus flumazenil and glucose PET in children with extratemporal lobe epilepsy. Neurology 2000; 54: 171–9.

Olsen RW, McCabe RT, Wamsley JK. $GABA_A$ receptor subtypes: autoradiographic comparison of GABA, benzodiazepine and convulsant binding sites in rat central nervous system. J Chem Neuroanat 1990; 3: 59–76.

Raymond AA, Fish DR, Sisodiya SM, Alsanjari N, Stevens JM, Shorvon SD. Abnormalities of gyration, heterotopias, tuberous sclerosis, focal cortical dysplasia, microdysgenesis, dysembryoplastic neuroepithelial tumour and dysgenesis of the archicortex in epilepsy. Clinical, EEG and neuroimaging features in 100 adult patients. [Review]. Brain 1995; 118: 629–60.

Richardson MP, Koepp MJ, Brooks DJ, Fish DR, Duncan JS. Benzodiazepine receptors in focal epilepsy with cortical dysgenesis: an ^{11}C-flumazenil PET study. Ann Neurol 1996; 40: 188–98.

Richardson MP, Friston KJ, Sisodiya SM, Koepp MJ, Ashburner J, Free SL, et al. Cortical grey matter and benzodiazepine receptors in malformations of cortical development. A voxel-based comparison of structural and functional imaging data. Brain 1997; 120: 1961–73.

Richardson MP, Koepp MJ, Brooks DJ, Duncan JS. ^{11}C-flumazenil PET in neocortical epilepsy. Neurology 1998; 51: 485–92.

Robb RA, Hanson DP. A software system for interactive and quantitative visualization of multidimensional biomedical images. Australas Phys Eng Sci Med 1991; 14: 9–30.

Rojiani AM, Emery JA, Anderson KJ, Massey JK. Distribution of heterotopic neurons in normal hemispheric white matter: a morphometric analysis. J Neuropathol Exp Neurol 1996; 55: 178–83.

Ryvlin P, Bouvard S, Le Bars D, De Lamérie G, Grégoire MC, Kahane P, et al. Clinical utility of flumazenil-PET versus [^{18}F] fluorodeoxyglucose-PET and MRI in refractory partial epilepsy. A prospective study in 100 patients. Brain 1998; 121: 2067–81.

Ryvlin P, Bouvard S, Le Bars D, Mauguiere F. Transient and falsely lateralizing flumazenil-PET asymmetries in temporal lobe epilepsy. Neurology 1999; 53: 1882–5.

Savic I, Persson A, Roland P, Pauli S, Sedvall G, Widen L. In-vivo demonstration of reduced benzodiazepine receptor binding in human epileptic foci. Lancet 1988; 2: 863–6.

Savic I, Ingvar M, Stone-Elander S. Comparison of ^{11}C-flumazenil and ^{18}F-FDG as PET markers of epileptic foci. J Neurol Neurosurg Psychiatry 1993; 56: 615–21.

Savic I, Thorell JO, Roland P. [^{11}C]flumazenil positron emission tomography visualizes frontal epileptogenic regions. Epilepsia 1995; 36: 1225–32.

Sperk G, Schwarzer C, Tsunashima K, Kandlhofer S. Expression of $GABA_A$ receptor subunits in the hippocampus of the rat after kainic acid-induced seizures. Epilepsy Res 1998; 32: 129–39.

Spreafico R, Battaglia G, Arcelli P, Andermann F, Dubeau F, Palmini A, et al. Cortical dysplasia. An immunocytochemical study of three patients. Neurology 1998; 50: 27–36.

Szelies B, Weber-Luxenburger G, Pawlik G, Kessler J, Holthoff V, Mielke R, et al. MRI-guided flumazenil- and FDG-PET in temporal lobe epilepsy. Neuroimage 1996; 3: 109–18.

Taylor DC, Falconer MA, Bruton CJ, Corsellis JA. Focal dysplasia of the cerebral cortex in epilepsy. J Neurol Neurosurg Psychiatry 1971; 34: 369–87.

Thom M, Sisodiya SM, Harkness WF, Scaravilli F. Microdysgenesis in temporal lobe epilepsy: a quantitative and immunohistochemical study of white matter neurones. Brain 2001; 124: 2299–309.

Van Paesschen W, Connelly A, King MD, Jackson GD, Duncan JS. The spectrum of hippocampal sclerosis: a quantitative magnetic resonance imaging study. Ann Neurol 1997; 41: 41–51.

Verhoeff NP, Petroff OA, Hyder F, Zoghbi SS, Fujita M, Rajeevan N, et al. Effects of vigabatrin on the GABAergic system as determined by [^{123}I]iomazenil SPECT and GABA MRS. Epilepsia 1999; 40: 1433–8.

Woermann FG, Barker GJ, Birnie KD, Meencke HJ, Duncan JS. Regional changes in hippocampal T2 relaxation and volume: a

quantitative magnetic resonance imaging study of hippocampal sclerosis. J Neurol Neurosurg Psychiatry 1998; 65: 656–64.

Woods RP, Mazziotta JC, Cherry SR. MRI-PET registration with automated algorithm. J Comput Assist Tomogr 1993; 17: 536–46.

Worsley KJ, Evans AC, Marrett S, Neelin P. A three-dimensional statistical analysis for rCBF activation studies in human brain. J Cereb Blood Flow Metab 1992; 12: 900–18.

Worsley KJ, Marrett S, Neelin P, Vandal AC, Friston KJ, Evans AC. A unified statistical approach for determining significant signals in images of cerebral activation. Hum Brain Mapp 1996; 4: 58–73.

Received August 6, 2001. Revised March 19, 2002.
Accepted May 2, 2002